

FINES EROSION: THE COUNTER-INTUITIVE EFFECT OF TURBULENCE

Joan A. R. BOULANGER^{1*}, Chong Y. WONG¹,
M S Amir ZAMBERI², S N Amira SHAFFEE², Zurita JOHAR³ and Maharon JADID³

¹CSIRO Mineral Resources, Clayton, Victoria 3169, AUSTRALIA

²Group Technical Solution PETRONAS, MALAYSIA

³ PETRONAS Carigali Sdn Bhd, MALAYSIA

* Corresponding author, E-mail address: Joan.Boulanger@csiro.au

ABSTRACT

Enabling the turbulent dispersion in a Computational Fluid Dynamics simulation of a liquid-solid flow through a pipe leads to a focus of low-Stokes number particles around the centreline of the pipe. This phenomenon is found to concentrate their impacts on a centrally located target surface such that a local and dense spot of erosion develops. This result is counter-intuitive as low-Stokes particles, by definition, follow the carrier average streamlines, which diminishes their probability of impact on a wall or bluff-body. Long straight piping systems are typical candidates to exhibit this phenomenon as turbulent pipe flows are characterized by an annular zone of turbulence that tends to disperse fine particles towards the centreline where they concentrate. Slurry erosion experiments on a cross-flow cylinder in a long straight pipe rig for a range of particle sizes confirm the occurrence of erosion focus as the size decreases, to which this phenomenon of turbulence-induced concentration is likely to contribute.

NOMENCLATURE

D rig diameter
 L cylinder diameter
 V carrier bulk velocity

d dispersed diameter
 d subscript, dispersed
 St Stokes number
 t subscript, turbulence

Δ difference operator
 α impact angle
 β azimuthal angle
 μ dynamic viscosity
 ρ density

$\langle \rangle$ averaging operator
 50 subscript, population median

INTRODUCTION

Erosion/wear is a major concern in modern industrial economies as it impacts in value for overall 5% of the domestic product (Agence Rhône-Alpes pour la Maîtrise des Matériaux, 1995), a non-negligible share of the wealth produced. Processing and resources industries are particularly exposed to the transport of abrasive particles as well as components of oil and gas wells. The physical properties of the carrier fluid in the case of slurries and the filtering systems retaining the biggest particles in general lead to a mechanism of transport for the dispersed material in which the drag of the

carrier closely drives the trajectories. For this reason, it has been often stated that the flow features have a mitigating effect on erosion by deviating the small particles from impact (Barton, 2003). However, some experimental results suggest that the scenario may not be so simple. For instance, Schweitzer and Humphrey (1988) glass beads / air experiments show that particles of small size tend to impact towards the centre of a cross-flow cylinder in a straight wind tunnel.

To quantify the amplitude of the response of a particle to drag by its carrier, a non-dimensional number, weighting the balance between a particle inertia and the drag it is subject to – when assumed spherical and in the Stokes regime - has been created and named the Stokes number (St):

$$St = \frac{V\rho_p d^2}{L18\mu} \quad (1)$$

with V being the bulk velocity of the carrier approaching the target of characteristic dimension L , ρ_p , the dispersed density, d , its diameter (under the spherical shape approximation), and μ the carrier viscosity. A high Stokes number means that particles have a large inertia relative to their drag and travel in a ballistic mode. At low Stokes number, particles are strongly influenced by the carrier drag. In practice, the particles and carrier rarely interact in the Stokes regime; nevertheless, the Stokes number is able to illustrate the main trends, generally.

Literature Review

Mechanisms of erosion by transported abrasive particles are split into two categories: direct and random impingement (Bai and Bai, 2012). Direct impingement happens when particles have sufficient momentum to traverse the streamlines at a flow re-direction location. This is concerned with high-Stokes particles, that is, particles on which insufficient drag can be applied by the carrier to redirect them due to their intrinsic inertia. Random impingement, on the contrary, addresses low-Stokes dispersed material in a turbulent flow: the particles are here sufficiently reactive to the drag of the carrier to respond to any of the random motions of the turbulence. Near a wall, although the carrier streamlines on an averaged basis would not lead to wall impact, these slight turbulence-induced excursions away from the main trajectory cause the particles to hit the wall randomly. This is an example of a counter-intuitive effect of the turbulence on fines erosion: low-Stokes particles generate erosion from a random motion while high-Stokes particles, in line with the flow axis, do not because of their high inertia that makes them insensitive to turbulence.

Another counter-intuitive effect on erosion of low-Stokes particles combined with particular flow structures is the vortex erosion phenomenon. A vortex entraps low-Stokes particles

and, if close enough to a wall, generates erosion spots in unsuspected areas (Brown, 2006).

The so-called fluid effect, that is, the deviation imposed by the drag of the fluid on the small particles at the wall approach, has been proposed as an explanation for erosion impact velocity dependency that differs from the kinetic energy concept (i.e. a velocity exponent differing from the response of erosion to impact kinetic energy) (Laitone, 1979). Vacuum experiments also report this kind of velocity dependency (Tilly and Sage, 1970) and the interpretation in this latter reference is an enhanced erosion from secondary impacts of large-then-fractured particles. It has also been proposed as an explanation for the apparent size threshold effect between two types of erosion mechanisms (Clark and Hartwich, 2001), that is from direct impact for large particles towards wet abrasion when small particles are trapped by the streamlines bathing the target (Stack and Pungiwat, 1999).

If, in general, fluid effect is considered to mitigate erosion occurrence, it may also be responsible for enhanced erosion on specific hot spots because of an insufficient drag of the flow streamlines that cannot make the particles completely avoid the wall but rather concentrate them at a specific impact location (plug tee, (Det Norske Veritas, 2007), cross-flow cylinder (Solnordal et al., 2013)). Nevertheless, the fluid effect precludes impact on a ballistic mode and induces side deviation following carrier streamlines along walls that modifies the impact rate, velocity and angle (Lyon et al., 1991), (Elfeki and Tabakoff, 1987), (Jordan, 1998).

Rationale

As explained in the introduction, Schweitzer and Humphrey (1988) revealed that particles transported in a straight pipe focus their impact at the centre of a cross-flow cylinder. This is a phenomenon that the present authors have observed as well: in a real rig similar to the one numerically studied in the following, a binary flow made of water loaded with sand was circulated. Slurry experiments were performed at Reynolds number 313,000 with two particle characteristic sizes ($d_{50} = 25 \mu\text{m}$ and $170 \mu\text{m}$ giving d_{50} -based Stokes number $St_{50} = 0.0353$ and 6.93 , respectively). The erosion hot spots on a cross-flow cylinder target were observed to move towards the centre when the particle size decreased, Figure 1.

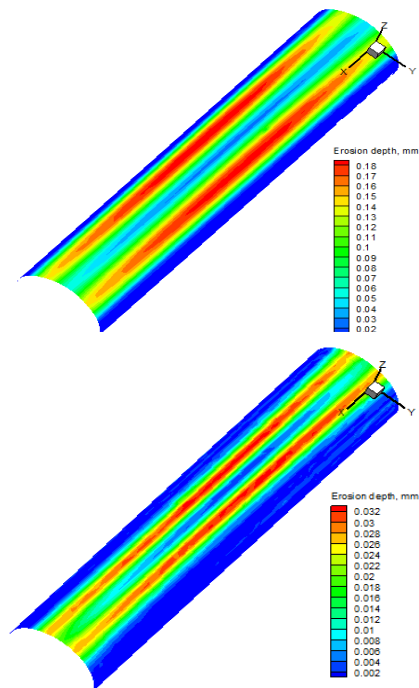


Figure 1: Laboratory slurry erosion experiments on a cross-flow cylinder in a straight pipe rig with two sand sizes. Top: $St_{50} = 0.0353$. Bottom: $St_{50} = 6.92$.

Experimental observations suggesting a narrowing of the impact zone around the stagnation line of a cross-flow cylinder subject to straight pipe binary flow when the particle size decreases cannot be easily explained by the general understanding of the fluid mechanical effect on low-Stokes particles. This warrants a thorough investigation of the phenomenon. Beyond the scientific novelty, the practical impact of exotic erosion wear not anticipated by state-of-the-art engineering practices on expensive and sensitive facilities like deep-water completions is of importance: these are instances where transported sand size is typically limited by retention systems (Zhang et al., 2007) and are primarily made of flows in pipe sections. Although these are mostly multi-phase systems, a first understanding of this phenomenon in binary flow is necessary.

Objective

The present study aims at exploring the turbulence effect on the transport of fines by a carrier fluid that can contribute to their focus towards the centre of a cross-flow cylinder in a straight pipe.

Scope

This contribution addresses a generic problem to emphasise the phenomenon. A straight circular pipe conveying a particle flow homogeneously prepared is considered. The target is a cross-flow cylinder made of aluminium, located at a distance from the inlet point allowing full establishment of the flow. Series of CFD simulations are carried out for a parametric sensitivity study (particles and fluid properties are varied to cover a range of behaviours in the transport of the particles) in order to explore the effects of turbulence on the concentration of the particles. These effects are assessed using the predicted erosion distribution on the target and the trajectory patterns of the particles. The other effect likely to contribute to concentrating particles in the centre of the pipe is aerodynamical lift, due to velocity gradients near the wall. This is a well understood effect and is not investigated in the present contribution.

Overview

After a general presentation of the configuration investigated and of the set-up of the simulations, a detailed analysis of the interactions imposed by the carrier on the dispersed phase is performed. It will be seen that, by varying the fluid and particle properties, a range of Stokes numbers can be reached where particles are not only sensitive to the average flow but also to the carrier turbulence, the latter being able then to organise and concentrate the trajectories.

METHOD

Configuration

A numerical erosion pipe rig was made of a straight pipe 52.6 mm in diameter with the erosion target as an aluminium cross-flow cylinder, 10 mm in diameter. The cylinder was positioned about 40 rig diameters downstream of the inlet. Figure 2 provides a sketch of the geometry simulated.

Simulations allowing for variation in bulk flow velocities, fluid properties and particle diameters were explored to cover a range of Stokes numbers and associated behaviours.

Mesh

The mesh of the flow domain was comprised of structured, unstructured and prismatic regions to capture the salient flow features and was optimised for computational efficiency and accuracy. Skewness was below 0.7 and orthogonality larger than 0.5. The mesh independency was assessed based on the pressure drop across the rig with a Grid Convergence Index (Roache, 1994) $< 10\%$ and a selection of the mesh size such that the pressure drop value differed from

its Richardson extrapolation by less than 10%. Near wall regions were appropriately solved with a y^+ interval mostly comprised between 20 and 200 and a peak of eddy viscosity away from any wall by a minimum of five mesh elements. The mesh was carefully refined in the vicinity of the target to accurately resolve the carrier flow features driving the particles and erosion field, Figure 2.

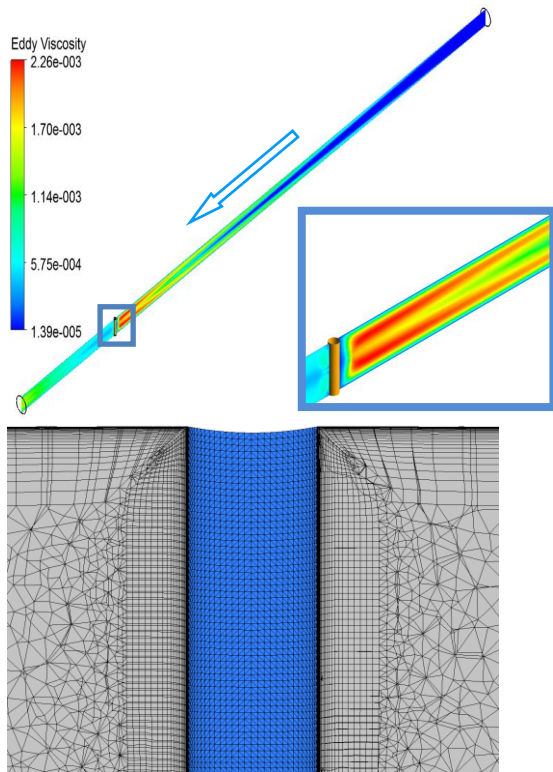


Figure 2: Top, rig sketch at a Reynolds number = 505,000. Bottom, mesh in the target vicinity.

Simulations

The simulations were carried out in double precision using ANSYS-CFX and the ANSYS Workbench tools for pre- and post-processing of the version 14.5. The fluid flow was modelled using the SST turbulence model with curvature correction. Particles, assumed spherical, were tracked as Lagrangian parcels and interacted with the fluid through Schiller-Naumann drag, turbulent dispersion (except when explicitly disabled), virtual-mass and pressure gradient forces. The inlet was of Dirichlet type with a velocity prescribed with a "1/7" turbulent profile, (De Chant, 2005), and particles were injected in equilibrium with the flow and uniformly across the inlet face. The turbulence intensity and eddy viscosity ratio at the inlet were taken at 5% and 10, respectively. The walls were numerically smooth with a restitution factor of 0.8 (Humphrey, 1990). The outlet was of Neumann type. All transport equations were solved with second-order accurate schemes. The carrier flow was converged first and then, particles were injected as a post-processing step to perform erosion prediction calculation. The distribution of erosion was collected on the surface of the target cylinder from a model calibrated for Garfield sand impacting an aluminium rod (Wong et al., 2012).

The iteration convergence was checked with insignificant changes found in the pressure drop when the residual tolerance was reduced by one order of magnitude. Conservation imbalances, including the parcels flux, were checked as virtually nil. Lagrangian solver statistical independency was reached using one million parcels released and with ten integration steps per cell element.

The CFD quality tests presented in this section and in the former Mesh Section were performed on the most relevant cases of the matrix of carrier/dispersed properties.

Output

Different combinations of dispersed size, carrier viscosity and density were investigated in order to visit a wide range of drag imposed to particles and therefore of Stokes behaviour. Erosion fields as predicted on the cross-flow cylinder were then analysed.

RESULTS

In a vacuum experiment, all the particles should travel ballistically. The angle of maximum erosion would therefore be determined by the angular dependency to erosion of the material and the geometrical projection of the dispersed flux density.

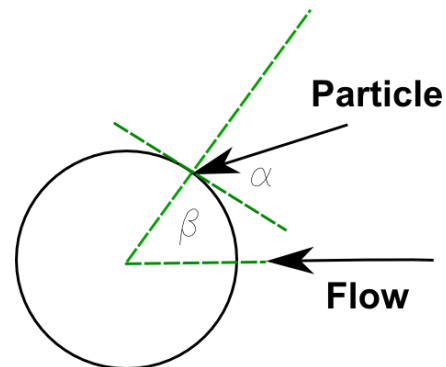


Figure 3: Coordinates system chosen along the cross-flow cylinder mid-line.

When particles are carried by a fluid, the inter-play between the particles and the streamlines going around the cylinder - the fluid effect - may change the location of the maximum erosion. $\Delta\beta$ is defined as the difference in cylinder angle β between the location of maximum erosion observed for a given flow and the one of a vacuum experiment taken as a reference. Figure 3 identifies the angles at use on the cross-flow cylinder. Positive angular difference $\Delta\beta$ means the location of maximum erosion is behind the reference one, following the direction of the flow. Figure 4 displays such angle shift for different cases of flow velocity, particle size and fluid properties translating into different Stokes numbers and associated effects of the carrier drag on a particle's trajectory. The angle shift is a non-monotonic function of the Stokes number. On the right end of Figure 4, $\Delta\beta$ is close to zero, in accordance with the fact that large-Stokes-number particles behave ballistically, are insensitive to fluid drag around the cylinder, and their impact characteristics are therefore almost identical to that of a vacuum experiment. With a decreasing Stokes number, $\Delta\beta$ drifts towards a positive value: this is the fluid effect. These particles are responsive to the drag of the fluid as it goes around the bluff body and do not impact in line with their far-field trajectory but somewhat behind. However, further decreasing the Stokes number of the impacting particles, $\Delta\beta$ follows a bell-shape function (authors' interpretation superimposed as a blue dashed line on Figure 4) and eventually becomes negative. This signifies that the corresponding impacts are happening closer to the centre of the target. This cannot be explained by the general interpretation of the fluid mechanics effect on low-Stokes particles.

In the following Figures 5 to 7, the erosion rate (aka erosion ratio) is made non-dimensional from the solid mass flux density homogeneously injected on the inlet cross section of the rig.

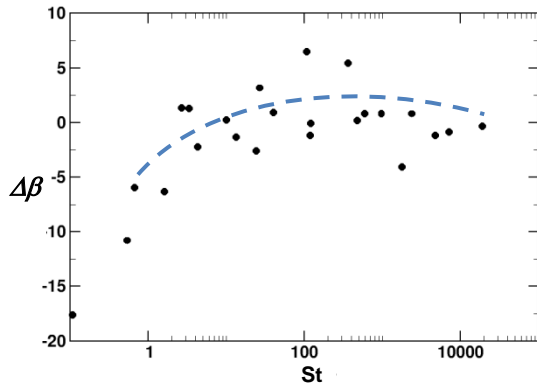


Figure 4: Angular shift $\Delta\beta$ of the maximum erosion location vs Stokes number. Particle/carrier density ratio = 53.

Two kinds of erosion fields are displayed in Figure 5 and Figure 6 for large and small particle Stokes numbers of 18800 and 4.24, respectively. Consistently with the angular shift of the maximum erosion location Figure 4, the erosion of low-Stokes particles is local, at the centre of the target, and dense compared to the high-Stokes configuration. However, the important fact at this stage is that this is not the case when the turbulence particle dispersion force is switched off, Figure 7. The level of the erosion peak is also, in this case, more in accordance with the fluid effect interpretation that anticipates a lower material loss when small particles are moved away from the target by the carrier fluid.

A sample of low-Stokes particle trajectories as they travel from their injection points is provided in Figure 8. These figures aim at emphasising the evolution of the cloud of small particles. Consistently with the previous findings, particles paths tend to concentrate in a narrow volume around the pipe axis as they approach the erosion target. The “turbulence noise” is perceptible in the snaking patterns induced.

A distribution of the turbulence activity in the pipe rig is visible in the form of a mid-plane cross section of the eddy viscosity field in Figure 2. The eddy viscosity has an annular distribution following the axis of the pipe. The eddy viscosity is made non-dimensional using, respectively, the carrier density and bulk velocity, and pipe rig diameter according to $\mu_t / (\rho V D)$, with μ_t the eddy dynamical viscosity, and ρ the carrier density.

Locally averaged impact angles of low- and high-Stokes particles are provided in Figure 9 for different cylinder angles β (see Figure 3 for β definition). While the high-Stokes particles verify the expected relationship $(\alpha + |\beta|) / \pi = 0.5$ that pertains to ballistic trajectories following the pipe axis (Solnordal and Wong 2012), the impact angle α for lower-Stokes particles drops quickly away the stagnation line. This is the classical effect of the fluid mechanics, preferentially deviating low-Stokes particles.

DISCUSSION

The current understanding of the fluid effect on fine particles approaching a target is that the latter are decelerated and deviated due to the action of the carrier going around the obstruction. This is explained by the important drag characteristic of low-Stokes particles that forces them to follow the carrier streamlines.

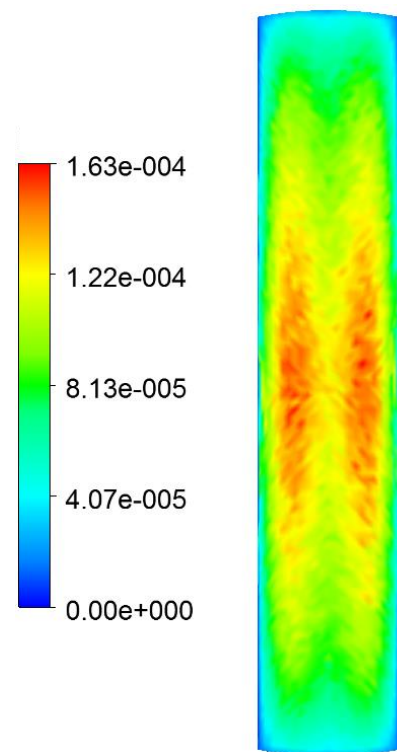


Figure 5: Erosion ratio distribution [kg/kg], $St = 18800$, particle/carrier density ratio = 2210.

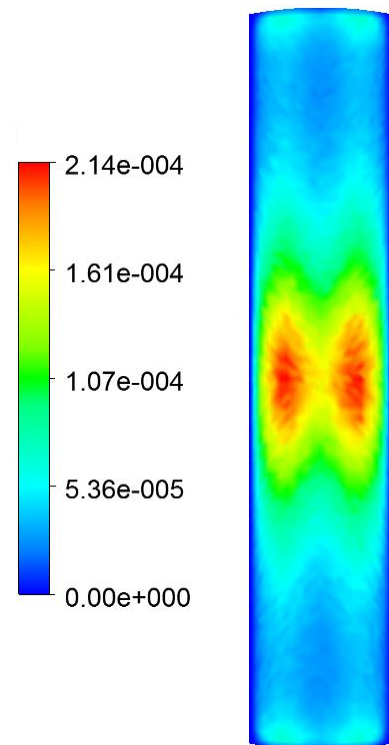


Figure 6: Erosion ratio distribution [kg/kg], $St = 4.24$, particle/carrier density ratio = 2210.

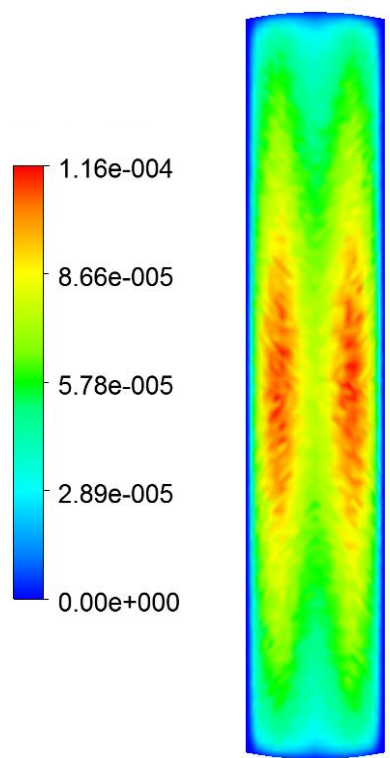


Figure 7: Erosion ratio distribution [kg/kg], $St = 4.24$, particle/carrier density ratio = 2210. Particle turbulent dispersion switched off.



Figure 8: Low-Stokes (4.24) particle tracks clustering in the neighbourhood of the pipe axis. Particle/carrier density ratio = 13.3.

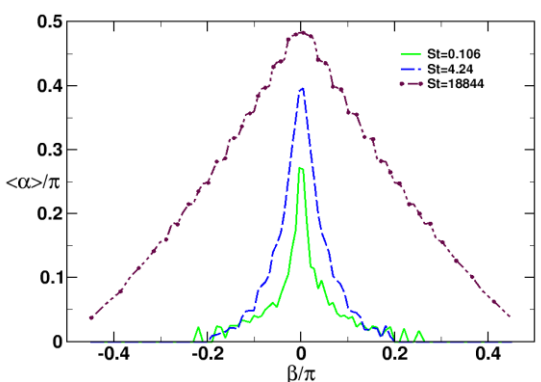


Figure 9: Average angle of impact at different azimuthal locations on the cylinder mid-line. Particle/carrier density ratio = 13.3.

As a consequence, the impact number and velocity are expected to decrease near the stagnation region while the deviated particles impact further downstream or not at all. Hence, for low-Stokes particles, the maximum erosion location tends to drift downstream on the cylinder. Figure 4, capturing the angular location change of the maximum erosion spot vs the impacting particles Stokes number, exhibits

effectively this behaviour but only for a range of Stokes number. Below this range, on the contrary, the maximum erosion location tends to move progressively closer to the stagnation point as the particle Stokes number further decreases. This is a break-down of the interpretations of the fluid mechanics effect on small particles. On the other hand, this is confirmed by experimental observations as reported in the Introduction section.

Interestingly, the target exposed surface erosion distribution for low Stokes number, Figure 6, reveals that the erosion field concentrates on the centre of the target in both directions and not only from an angular point of view along the cylinder mid-line. This can be explained only by a focus of the particle trajectories and subsequent impacts. Hence, the apparent angular shift of the maximum erosion point back towards the stagnation region of the cylinder in the lower range of the Stokes number as discussed in Figure 4 is in fact the consequence of this general focus of the erosion damage. Furthermore, this focusing effect disappears when the turbulence dispersion acting on the particles is switched off as a model in the simulations as shown on the erosion field displayed in Figure 7.

Investigations of the history of low-Stokes particles in Figure 8 reporting their trajectory along the pipe show that the particle paths slowly drift towards the pipe centre such that the flux of particles which was initially injected homogeneously across the cross-section of the pipe rig becomes denser near the pipe axis, and therefore near the target centre, as the latter is approached. This mechanism is a good candidate to contribute to the experimental observations reporting that low-Stokes particles may tend to create erosion spots near the centre of a cylinder in cross-flow as discussed earlier.

It is admitted, (Humphrey, 1990), that particles transported in a turbulent flow are subject to something analogous to positive thermophoresis, that is, they are dispersed by turbulence from regions of high agitation towards more quiescent regions. The mid-plane cut view of the pipe rig of turbulent viscosity in Figure 2 shows that the pipe flow structure typically organises an annular volume of turbulence, relatively close to the wall, which, according to the thermophoresis-like mechanism, should tend to disperse the particles towards the pipe axis. For a given pipe length, preferentially low-Stokes particles are responsive enough to lend themselves significantly to this turbulence re-organisation of their path. This is effectively what is reported in the preceding results and explains that this counter-intuitive erosion focus is essentially observed with the smallest particles in the present contribution. From a practical point of view, it is then important to remark that this is the overall design of the facility upstream of the target that offers the opportunity for the turbulence to progressively focus the particle paths and create a localised, dense erosion spot.

This phenomenon is not incompatible with the more classical fluid effect deviating low-Stokes particles near the target as it could have first appeared. Both super-impose, actually: although the turbulent dispersion pushes the particles towards the axis during their journey in the upstream pipe, they are still deviated when close to the target. As evidenced in Figure 9, providing the average impact angle with respect to the location on the mid-line of the cylinder, away from the stagnation point, the typical average angle of impact falls sharply for low-Stokes particles, indicating that particles are deviated by the flow and are grazing the cylinder surface. On the other hand, large-Stokes particles are shown, on this same figure, obeying the ballistic mode, as expected.

Figure 10 illustrates the combination of both the turbulence dispersion and fluid mechanics effects on low-Stokes particles carried in a straight pipe and impacting a cross-flow cylinder.

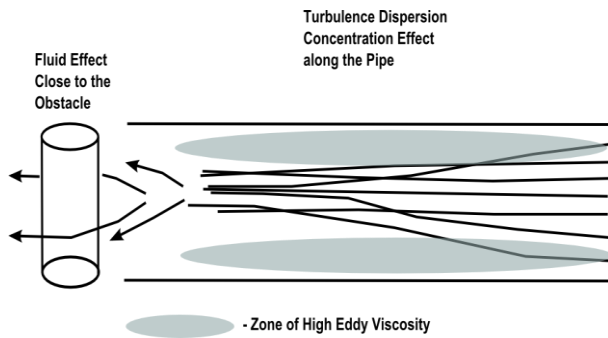


Figure 10: Interpretation of the turbulence dispersion and fluid mechanics effect on fines carried in a straight pipe flow towards a cross-flow cylinder.

CONCLUSION

- In a fluid able to occasion significant drag on the carried abrasive particles, the latter tend to be deviated by the streamlines when approaching a wall and follow the fluid, avoiding the impact. This is the well-known fluid effect. This effect is driven by the average flow structures (streamlines based on the average flow velocity).
- On the other hand, such a fluid is able, once again through its enhanced drag, to transfer the turbulence to the cloud of particles. Following a dispersion process similar to positive thermophoresis, these latter tend to depart from an area of high turbulence level and cluster into low-turbulence volumes.
- In the case of a flow along long straight pipe sections in which the turbulence agitation is preferentially located in an annular zone, this turbulent dispersion process focuses the particle streams on the centreline. At the impact, this tends to create local, dense erosion spots.
- Both the fluid effect and this turbulence dispersion effect combine. They nevertheless act at different scales. The classical fluid effect is mostly governed by the fluid spatial scales immediately around the target. The turbulence dispersion effect is a more progressive process, acting, for instance, on long straight pipe binary flows as studied here.

ACKNOWLEDGEMENT

The authors acknowledge financial support and permission from PETRONAS Carigali Sdn. Bhd. to publish some of the results of this contribution. The authors also acknowledge the appropriation funding from CSIRO for the generation of additional results and the manuscript preparation. The authors are grateful to CSIRO and external reviewers for their suggestions.

REFERENCES

- Agence Rhône-Alpes pour la Maîtrise des Matériaux, (1995), "Rapport de synthèse endommagement des matériaux par abrasion".
- BAI, Y. and BAI Q., (2012), "Subsea engineering handbook", Gulf Professional Publishing, Paris, France.
- BARTON, N. A., (2003), "Erosion in elbows in hydrocarbon production systems: review document", *Research Report TÜV NEL Limited*, Glasgow, UK.
- BROWN, G., (2006), "Use of CFD to predict and reduce erosion in an industrial slurry piping system", *Int. Conf. CFD in Process Ind.*, Melbourne, Australia, December 13-15.
- CLARK, H. M., and HARTWICH R. B., (2001), "A re-examination of the particle size effect in slurry erosion", *Wear*, **248**, 147-161.

DE CHANT, L. J., (2005), "The venerable 1/7th power law turbulent velocity profile: a classical nonlinear boundary value problem solution and its relationship to stochastic processes", *App. Math. Comput.*, **161**, 463-474.

DET NORSKE VERITAS, (2007), "Recommended practice RP 0501 erosive wear in piping systems".

ELFEKI, S. and TABAKOFF W., (1987), "Erosion study of radial flow compressor with splitters", *Comput. Fluids*, **109**, 62-69.

HUMPHREY, J. A. C., (1990), "Fundamentals of fluid motion in erosion by solid particle impact", *Int. J. Heat Fluid Flow*, **11**, 170-195.

JORDAN, K., (1998), "Erosion in multiphase production of oil & gas", *Int. Corrosion Conf. Expo.* San Diego, USA, March 22-27.

LAITONE, J. A., (1979), "Aerodynamic effects in the erosion process", *Wear*, **56**, 239-246.

LYON, R. S., WONG K. K. and CLARK H. M., (1991), "On the particle size effect in slurry erosion", *Wear*, **149**, 55-71.

ROACHE, P. J., (1994), "Perspective: a method for uniform reporting of grid refinement studies", *J. Fluids. Engng*, **116**, 405-413.

SCHWEITZER, M. O. and HUMPHREY J. A. C., (1988), "Note on the experimental measurement of particles embedded in one and two in-line tubes in a high speed gas stream", *Wear*, **126**, 211-218.

SOLNORDAL, C. B. and WONG C. Y., (2012), "Predicting surface profile evolution caused by solid particle erosion" *Int. Conf. CFD in Process Ind.*, Melbourne, Australia, December 10-12.

SOLNORDAL, C. B., WONG C. Y., ZAMBERI A., JADID M. and JOHAR Z., (2013), "Determination of erosion rate characteristic for particles with size distributions in the low-Stokes number range", *Wear*, **305**, 205-215.

STACK, M. M. and PUNGWIWAT N., (1999), "Slurry erosion of metallics, polymers, and ceramics: particle size effects", *Mat. Sci. Tech.*, **15**, 337-344.

TILLY, G. P. and SAGE W., (1970), "The interaction of particle and material behaviour in erosion processes", *Wear*, **16**, 447-465.

WONG, C. Y., SOLNORDAL C. B., SWALLOW A., WANG S., GRAHAM L. and WU J., (2012), "Predicting the material loss around a hole due to sand erosion", *Wear*, **276-277**, 1-15.

ZHANG, .Y, REUTERFORS E. P., MCLAURY B. S., SHIRAZI S. A. and RYBICKI E. F., (2007), "Comparison of computed and measured particle velocities and erosion in water and air flows", *Wear*, **263**, 330-338.